



Oct 23rd, 12:00 AM

Effective Width in Elastic Post-buckling of Thin Flanges

Robert W. Dannemann

Follow this and additional works at: <https://scholarsmine.mst.edu/isccss>



Part of the [Structural Engineering Commons](#)

Recommended Citation

Dannemann, Robert W., "Effective Width in Elastic Post-buckling of Thin Flanges" (1990). *International Specialty Conference on Cold-Formed Steel Structures*. 1.

<https://scholarsmine.mst.edu/isccss/10iccfss/10iccfss-session3/1>

This Article - Conference proceedings is brought to you for free and open access by Scholars' Mine. It has been accepted for inclusion in International Specialty Conference on Cold-Formed Steel Structures by an authorized administrator of Scholars' Mine. This work is protected by U. S. Copyright Law. Unauthorized use including reproduction for redistribution requires the permission of the copyright holder. For more information, please contact scholarsmine@mst.edu.

EFFECTIVE WIDTH IN ELASTIC POST-BUCKLING OF THIN FLANGES

by Robert W. Dannemann

1) INTRODUCTION

The effective width (EW) concept is a classical resource for representing local buckling effects on stiffened flat steel flanges. There has been a great deal of testing and investigations on this matter and in the last decade also unstiffened flanges and webs of beams were included in this technique by the codes.

The most important contribution to the adoption of this method was Prof. George Winter's proposal (1) included by AISI in their Specification of Light Gage Structural Members of 1946.

As known, the EW concept is based on Von Karman's proposition of 1932 where the uneven stress distribution of buckled flanges were replaced by evenly stressed fictitious strips along corners of the flanges. This structural artifice has shown excellent results in design practice of metal structures. A great number of tests in different countries confirms the accuracy of this method mainly in plates buckling in the inelastic range, but from time to time some discrepancies have been detected and published for flanges buckling elastically.

In this paper the author presents, based on tests performed on thin trapezoidal sheets, a complementary criteria for EW, when flanges buckle in the elastic range. This method compares well with the observed behavior and ultimate strength of test specimens. The author's suggestion is that for inelastic buckling the AISI and correlated design codes are valid but when sheets are very slender and they buckle elastically a modified EW criteria be applied. This proposed method not only shows excellent correlation with tests, but also facilitates a rational agreement between stiffened and unstiffened flange behavior when plates are very thin, fulfilling physical requirements not accomplished by the classical EW method, as it will be demonstrated in the paper.

2) DESCRIPTION OF TESTS

During 1988/89 the author had the opportunity to monitor a test program of trapezoidal sheets, for the purpose of issuing allowable load tables for an important roofing sheet industry. Over 70 sheets were submitted to destructive bending tests according to the test layout shown on Fig. 1a. To avoid the flattening of sheets during loading, transversal steel strips were fastened to the upper flanges, as shown on Fig. 1b.

1. Civil Engineer, Consultant, Santiago, Chile, Eng. Manager PUGA MUJICA Assor. SA

In this paper only a limited number of specimens of the sheets shown on Fig. 2 will be analyzed, because these sheets show the most important differences between calculated and tested ultimate strength.

The value P_{ua} is the ultimate load calculated according to the 1986 AISI Specification, and P_{ut} is the measured test ultimate load. Only the thinner sheets of 0.55 mm (BWG 24) and 0.40 mm (BWG 27) thickness are reported here because thicker sheets showed good agreement with code values. Values P_{ua} and P_{ut} are listed on Table 1. The theoretical value of P_{ua} was calculated by the following expression:

$$P_{ua} = \frac{8 \cdot S_e \cdot F_y}{L} \quad (1)$$

Where S_e is the effective section modulus of the sheet when the extreme fiber is compressed to F_y , calculated following the 1986 AISI Specification.

The values of Table 1 show differences in the order of 45% for the BWG 27 and 27% for the BWG 24 sheets, demonstrating that the calculated values are on the unconservative side. This result was considered as not satisfactory and it was decided to investigate this rather high level of discrepancy between theoretical and tested values.

3) BEHAVIOR OF ELASTICALLY BUCKLED FLANGES

During testing, the trapezoidal sheets buckled in the compression flange and compression portion of the web typical of a bending member; however, several observations can be made regarding the member's behavior.

At the load corresponding to the theoretical critical buckling stress for the flange, instantly a set of very regular shaped bulbs and depressions appeared in the flange and web. This buckling appeared in the center portion of the test specimen between both load applications, as shown on Fig. 3. It was remarkable that the web deformations extended over the entire depth, not over a partial web depth, as is described by current codes. When the sheets were unloaded, the local deformations disappeared immediately with no remainder of deformations, thus confirming the elastic buckling behavior.

For all test specimens, when the ultimate load was reached, it was observed that the sheets collapsed locally, folding in a very uniform way, as shown by Fig. 4. This suggests that a defined failure mechanism was acting, which followed definable rules that produce the same collapse mode. The failure mechanism was not sudden thus giving the impression that a local yielding process was acting. Actually, the author found the failure pattern to be similar to the failure patterns shown in Refs. 14 and 16.

From the above observations the following conclusions were driven:

- a) Two completely different phases exist in the structural response of the sheet, one before and another after reaching the critical buckling load of the flanges.
- b) The critical buckling load of the flanges defines a point of change in the physical behavior.
- c) Almost simultaneously, the flanges and webs buckled when the critical load was reached. The buckling was a snap through like action, where

circular bulbs and depressions appeared on their faces in a strictly regular and periodic pattern. Interaction and sympathetic action between flanges and webs becomes evident.

- d) The local buckling deformations were perfectly elastic.
- e) The failure of the sheets was produced by local folding of the flanges in a uniform collapse mechanism where the sheets were stressed longitudinally and transversally in bending and axially, plus possible local inelastic buckling.

Based on these observations the author concluded that the failure of these sheets, when subjected to bending, should be represented by two strength components. The first component is the total section stressed to the critical buckling stress. An additional component is represented by the strength of the corners and their adjacent parts. Ultimate strength may be obtained by adding both components based on the principle of superposition.

4) INVESTIGATION

The investigation to determine the real physical behavior of elastically locally buckled flanges of corrugated sheets in bending started with a bibliographic search. In Refs. 6, and 10 the EW criteria are critically analyzed and in Refs. 2, 11, and 13 alternative methods are presented. In Ref. 8 webs were included in the method and Refs. 7, 9, and 15 report unconservative results in the use of the classical EW criteria when compared with tests. Data on corner failure mechanisms can be found in Refs. 14, and 16, which probably will be useful in future studies for a better understanding of the collapse of the corners in elastically local buckled sheets.

Based on the analysis of the results, and the observation of the tests, taking into consideration the available literature, the author investigated a number of different approaches to explain the unpredictable results of the tests. Finally the author adopted the method described in this paper as the best fit to the test results and physical behavior.

5) PROPOSED METHOD

The structural response of elastically buckled flanges may be represented by two strength components, as follows:

- a) An overall basic strength given by the classical critical buckling stress distributed evenly over the whole width of the compressed element.
- b) An additional strength concentrated in the corners and narrow strips adjacent to same corners, when stressed to an average ultimate stress higher than the critical stress, but less than the yield limit of the steel.

In Fig. 5a, a flat stiffened element of width w is shown, and Fig. 5b shows the critical stress acting over the whole section.

For stiffened flanges the critical stress is:

$$f_c = \frac{K \pi^2 E}{12 (1-\mu^2) (w/t)^2} \quad (2)$$

For metric units (forces in KN and dimensions in cm) this expression becomes:

$$f_c = \frac{(137.8)^2}{(w/t)^2} \frac{K}{K} \quad (3)$$

In this loading stage the flange strength Q_u (excluding the corners to facilitate analysis) is:

$$Q_u = f_c w t \quad (4)$$

Surpassing this load the center of the plate, acting like a weak spring, because of its elastic buckling conformation, no longer will contribute to the strength and only narrow strips adjacent to the corners may contribute to increase the strength of the flange. In Fig. 5c the real uneven stress distribution shown in dotted lines may be replaced by an evenly distributed ultimate stress F_p over two "real" effective widths $B/2$ adjacent to the corners, equalling the areas under the curves. This additional strength ΔQ is:

$$\Delta Q = (F_p - f_c) B t \quad (5)$$

and the total strength Q_u of the flange will be:

$$Q_u = f_c w t + (F_p - f_c) B t \quad (6)$$

where B is the effective width, and F_p is the average ultimate stress in the corners. Both parameters should be defined to calculate Q_u .

After selecting this method as the most representative for the elastic local buckling of flanges, the author found that Prof. L.C. Maugh and L.M. Legatski (2) already in 1946 made a similar proposal. Consequently credit has to be given to these authors and following their recommendation for the maximum stress F_p , the author adopted the value of the proportional limit as 5/8 of corresponding yield limit.

The definition of the effective width B will be given in following chapters.

6) ULTIMATE COMPRESSION CAPACITY GRAPHS

The graphical representation of the ultimate compression load of a flange as a function of the width/thickness ratio is useful to help visualize some important facts about the post buckling behavior of very thin plates. The ultimate compression capacity Q_u calculated by the 1986 AISI Specification is:

$$Q_u = b t F_y \quad (7)$$

where b is the EW of the flange.

To simplify the analysis it will be assumed that the steel quality is constant ($F_y = 30 \text{ KN/cm}^2$). Later the influence of varying the yield limit will be shown by tracing a family of curves for different yield limits (Fig. 8).

In Fig. 6a a stiffened flange of width w is shown, which will be compared with the same flange but split in the middle, thus resulting in two unstiffened flanges of width $w/2$ each (Fig. 6b).

In Fig. 7 the ultimate compression capacity Q_u of these two cases are shown where:

Curve A B C D represent Q_u for the stiffened flange

Curve A E F G represent Q_u for the double unstiffened flanges.

These curves can be divided into three branches: the compact range, the inelastic buckling range and the elastic buckling range, as defined by the corresponding characteristic width/thickness ratios taken from the AISI Specification. For low w/t ratios $\lambda < 0.673$, the flanges are compact. When the value of Eq. 8 exceeds 0.673, with $k=4$ for a stiffened, and $k=0.43$ for an unstiffened flange, the inelastic buckling range starts, which passes to elastic buckling when the condition expressed in Eq. 9 is reached:

$$\lambda = \frac{1.052}{\sqrt{K}} \frac{w}{t} \sqrt{\frac{F_y}{E}} = 0.673 \quad (8)$$

$$\left(\frac{137.8}{(w/t)} \right)^2 K = F_p = (5/8) F_y \quad (9)$$

The corresponding (w/t) lim and (w/t) crit values are marked on both curves of Fig. 7.

Observing the curves it can be verified that both curves grow as the width to thickness ratio increases. When the w/t ratio tends to infinity that means t/w approaches zero and the following limit values of Q_u are attained:

$$\text{Stiffened flanges } Q_u = 50.28 F_y t^2 = 1,508 t^2 \quad (10)$$

$$\text{Unstiffened flanges } Q_u = 32.98 F_y t^2 = 989 t^2 \quad (11)$$

where Q_u is given in KN and t in cm

These values show that according to the classical EW criteria, in the limit, when the flange width is infinitely wide, stiffened flanges would have 52% more capacity to resist compression than same flange split at the middle, forming a pair of unstiffened flanges. The analysis of these results deserve the following comments:

- It is physically improbable that when compressed flanges buckle in the elastic range, its overall strength may increase, because the quadratic reduction in the buckling strength cannot be compensated by the linear increase of the area, thus producing a constrained reduction in the overall strength as the width increased (for constant thickness).
- It is physically improbable that the stiffened flange of Fig. 7, when w/t approaches infinity, will have more compression capacity than the double unstiffened flanges of the same width and area. It is obvious that when the width becomes very large, the critical stress contribution vanishes and the central part of the flange no longer contributes to the overall strength.

Based on these two observations the following conclusions may be drawn:

- Necessarily both curves ABCD and AEFG must converge to a common strength value when w/t becomes very large approximating infinity. They must

meet in definite value which is solely dependant on the corners strength.

- d) Curves ABCD and AEFG necessarily must have descending CD and FG branches.

7) REAL EFFECTIVE WIDTH

For the case of local elastic buckling the author defines a "real" EW designated with the letter B, which contrasts with the classical EW method, is a dimension of defined physical meaning. It does not come from empirical considerations and it is the measure of the integral of the overstressed areas of the corner strips provided a defined value F_p is established. For the case of elastic local buckling, it can be assumed that the contribution of the flats adjacent to the corners have an invariable width referred to the thickness of the plate, and independent of the stress level, provided that the critical buckling stress has been surpassed. This constant EW will be defined by the ratio B/t , independent of the width thickness ratio. Consequently when the width thickness ratio is very large, approximating infinity, the real effective width represents the ultimate strength of such flange with no buckling strength at all.

Based on the above reasoning the "real" EW may be obtained from the classical expression of the effective width for unstiffened flanges (12), with $k=0.43$

$$F_y = \frac{k \pi^2 E}{12(1-\mu^2)(B/t)^2} \quad (12)$$

The "real" EW is:

$$B = 180.6 \frac{t}{\sqrt{F_y}} \cong \frac{180}{\sqrt{F_y}} t \quad (13)$$

The same value is obtained from the expressions of the 1986 AISI Specification when $k=0.43$ and for $t/w=0$

$$B/2 = \rho w = \frac{1 - (0.22/\lambda)}{\lambda} \frac{w}{t} t \quad (14)$$

where value λ is calculated by Eq. 8

With this value of B Eq. 6 may be rewritten as follows:

$$Q_u = f_c w t + ((5/8) F_y - f_c) \frac{180}{\sqrt{F_y}} t^2 \quad (15)$$

$$Q_u = f_c ((w/t) - (180/\sqrt{F_y})) t^2 + 112.5 \sqrt{F_y} t^2 \quad (16)$$

By representing Eq. 16 in Fig. 7 with $F_y = 30 \text{ KN/cm}^2$, two transition curves indicated as branches CD' and FG' result, where points D' and G' meet at infinity.

The equations of these curves are, introducing the value $F_y = 30 \text{ KN/cm}^2$ into Eq. 16

$$\text{Stiffened flanges } Q_u = \left(\frac{137.8}{(w/t)} \right)^2 4 \left(\frac{w}{t} - 32.9 \right) t^2 + 616 t^2 \quad (17)$$

$$\text{Unstiffened flanges } Q_u = \left(\frac{137.8}{w/2t} \right)^2 0.43 (w - 32.9)t^2 + 616 t^2 \quad (18)$$

In these expressions, when t/w becomes zero the first term vanishes and only the second term stays, in this case $Q=616 t^2$ which is the strength of the corners alone. For one unstiffened flange alone the Eq. 18 converts to:

$$Q_u = \left(\frac{137.8}{w/t} \right)^2 0.43 (w/2t - 16.45) t^2 + 313 t^2 \quad (19)$$

It is convenient to represent curves for different steels. In Fig. 8 the compression capacity curves for three different steels are shown, allowing the visualization of the effects of the steel yield limit on the post buckling ultimate loads as a function of w/t . Figure 8 shows the increasing capacity of flanges in the inelastic range, the decreasing values for elastic locally buckled plates, and finally, the characteristic value when $t/w=0$ that is to say, when widths becomes extremely wide. Again, it is remarkable that in the inelastic range, the classical EW method furnishes correct results. On the contrary in the elastic range of local buckling these curves show significant differences with the classical EW method.

8) MODIFIED EW CRITERIA

The classical empirical criteria for EW assumes that the effective width b depends on a coefficient C defined by Winter (1), and adopted later with slight modifications by AISI and other codes. The term C is a linear function of the so called normalized slenderness $t/w \sqrt{E/f}$

This value was originally based on a randomly distributed set of tests results. The equation for C is:

$$C = 1.9 \left(1 - 0.415 \frac{t}{w} \sqrt{\frac{E}{F_y}} \right) \quad (20)$$

In Fig. 9 this equation is represented by the full line where for the ratio $t/w=0$ (infinite width of flange), the C value reaches its highest value $C=1.9$. By inverting the independent variable as shown in Fig. 10, the representation of C is improved. The postbuckling range is better represented than in Fig. 9 where, for the higher width/thickness ratios, only a very narrow space of the graphical representation is available.

In both Figs. 9 and 10 the parameter C appears as an increasing continuous function of the width/thickness ratio. But actually the passage from inelastic to elastic local buckling represents a physical discontinuity, which does not show on these curves. The same as in column buckling, the transition from the inelastic to elastic buckling is marked by a break in the physical phenomena and in its theoretical and graphical representation. The same must happen in plate buckling. Based on the above reasoning such a break point in the graphical representation of C may be found by calculating the value of B in the limit when $t/w=0$ applying Eq. 13

$$B = C t \sqrt{\frac{E}{F_y}} = \frac{180}{\sqrt{F_y}} t \quad (21)$$

Solving Eq. 20, the value C becomes 1.247, instead of 1.9, assumed in the current EW method. Observe that this limit value of C is independent of the steel quality. If it is assumed that in the inelastic range the actual value is correct, it is reasonable to trace a line XB as shown on Fig. 9 as

a first approximation of a modified value of C in the elastic buckling range. By introducing this modified C value, it will be possible to apply actual codes without changing the general method established for computing the EW of compressed flanges.

9) MODIFIED EW CRITERIA APPLIED TO BENDING

The modified criteria for the postbuckling strength of thin plates described above may be extended to the bending of corrugated sheets, as those used in the tests described in this paper.

When dealing with flanges and webs of trapezoidal sheets of width/thickness ratios higher than 50 or 60, and after observing the behavior of the tests, especially the web buckling of these sheets with its center of gravity near to the lower flanges, it was concluded that in the elastic range the web buckling extended on the whole width of the webs and not partially as it is deducted from EW criteria of the actual codes. The observed buckles in webs (bulbs and depressions) extend over the whole width, from corner to corner, and in accordance with this observation, when reaching the elastic critical stress level in the webs it is assumed that the entire web buckles. In this case partial buckling of the web is improbable because the deformation of the compressed part of the web may extend to the slightly tensioned lower edge. Consequently for the bending of the trapezoidal sheets of Fig. 2 with very wide lower flanges, in comparison to the upper ones, the "real" EW strips B/2 were assumed to be acting in the upper flanges and on the whole webs as shown in Fig. 11. In the case of the yield limit of 30 KN/cm² the value of B/2 will be 16.45t defining the "real" effective section as the one shown in Fig. 11. Based on this reduced section, the effective section Se' may be easily determined. The effective ultimate bending moment M_{up}, will be:

$$M_{up} = S f_c + ((5/8) F_y - f_c) S e' \quad (22)$$

where S = total section modulus (No discounts).
 Se' = "real" effective section modulus (based on Fig. 11)
 Both values are included in Table 2

In Table 2 the ultimate effective loads P_{up}, were calculated by the following expression:

$$P_{up} = 8 \frac{M_{up}}{L} \quad (23)$$

In Table 2 the value P_{up} is compared with the test values P_{ut}, and as it can be observed, very good agreement exists between tested and calculated values applying the proposed method.

It will be useful to mention that this method is not very sensitive to the adoption of either the maximum ultimate average stress F_p, or the "real" value of B/2. These differences only affect the corner strength, and not the basic strength which depends on the critical stress of buckling which is well defined when border conditions of the plates are known.

10) CONCLUSIONS

A rather simple method for post buckling strength evaluation of flange elastic buckling has been presented. This method is based on bending test results and studies on thin standard trapezoidal sheets. This method allows the calculation of the post buckling strength of flanges and webs by using physically measurable values instead of empirical parameters. These values are: the theoretical critical buckling stress f_c of the plate according to its border conditions, a constant so called "real" effective width B which varies slightly with the steel quality and a reduced maximum ultimate average stress F_p for the corner region (Less than yield limit).

The proposed method may be applicable for beams and columns, having stiffened or unstiffened flanges as well as webs. It may be used in combination with building codes, where this method only will be applicable for local buckling in the elastic range. For inelastic buckling building codes are totally valid.

This method can also be extended to partially stiffened flanges, but this will surpass the scope of this paper, and may deserve future publications.

Discussions and the critical review of this paper by the profession and future investigations will be welcome.

ACKNOWLEDGEMENTS

The tests described in this paper are part of a set of more than 70 destructive bending tests conducted by COMESI SAIC, the largest corrugated steel sheet producer of Argentina. These tests allowed the author the fulfillment of his investigation. The contribution of COMESI SAIC to the advance of steel technology is gratefully acknowledged.

APPENDIX I - REFERENCES

1. Winter, George, "Strength of Thin Steel Compression Flanges," Transactions ASCE, 1946.
2. Maugh, L.C. and Legatski, L.M., Discussion of ref. (1), Transactions ASCE, 1946.
3. American Iron and Steel Institute, "Specification for the Design of Cold Formed Structural Members," 1986.
4. Yu, Wei Wen, "Cold Formed Steel Design," Wiley Inter Science, New York, 1985.
5. Dannemann, R.W., "Anchos efectivos de elementos de chapa delgada," IX Jornadas Argentinas de Ingenieria Estructural, Buenos Aires, October 1989.

PAPERS published in the Proceedings of the INTERNATIONAL SPECIALITY CONFERENCES ON COLD FORMED STRUCTURES - University of Missouri-Rolla.

6. Lind, N.C., Ravindra, M.K., and Power, J.A., Review of the Effective Width Formula. 1st. Conference, 1971.
7. Bergfeld, A., Edlund, B., and Larson, H., Experiments on Trapezoidal Sheets in Bending. 3rd Conference, St. Louis, 1975.
8. LaBoube, R.A. and Yu, Wei Wen, Study of Cold Formed Steel Beams Webs Subjected to Bending Stress, 3rd Conference, St. Louis, 1975.

9. Baehre, R., Sheet Metal Panels for use in Building Construction, 3rd Conference, St. Louis, 1975.
- 10 Venkataramaiah, K.R., and Roarda, I., Local Buckling of Thin Walled Channels, 4th Conference, St. Louis, 1978.
- 11 Rhodes, J., Post Buckling Behaviour of Bending, 6th Conference, St. Louis, 1982.
- 12 Mulligan, G.P., and Pekoz, T., Analysis of Locally Buckled Thin Walled Columns, 7th Conference, 1984.
- 13 Rhodes, J., Treatment of Buckling in the New British Code, 8th Conference, St. Louis, 1986.
- 14 Key, P.W., Hasan, S.W., and Hancock, G.J., Column Behaviour of Cold Formed Hollow Sections, 8th Conference, St. Louis, 1986.
- 15 Pan, C.C. and Yu, Wei Wen, High Strength Steel Members with Unstiffened Compression Elements, 9th Conference, St. Louis, 1988.
- 16 Mahmood, H.F., and ABED, S.H., Computer Aided Analysis of Thin Walled Structural Components Subjected to Axial and Bending Crush Loads, 8th Conference, St. Louis, 1986.

APPENDIX II - NOTATIONS

b	effective width
B	"real" effective width
C	effective width coefficient
E	elasticity limit
f	stress
fc	critical buckling stress
Fp	proportional limit
Fy	yield strength
K	buckling coefficient
L	span
M _u	ultimate bending moment
P _u	ultimate load calculated by AISI criteria
P _p	ultimate load proposed in this paper
P _t	ultimate load obtained by tests
Q _u	ultimate flange strength excluded corners
S	total section modulus
S _e	effective section modulus as established by AISI
S _{e'}	"real" effective modulus proposed in this paper
t	sheet thickness
w	flange width
ΔQ	additional strength of corners strips
λ	slenderness factor (AISI 1986)
μ	Poisson modulus = 0.3

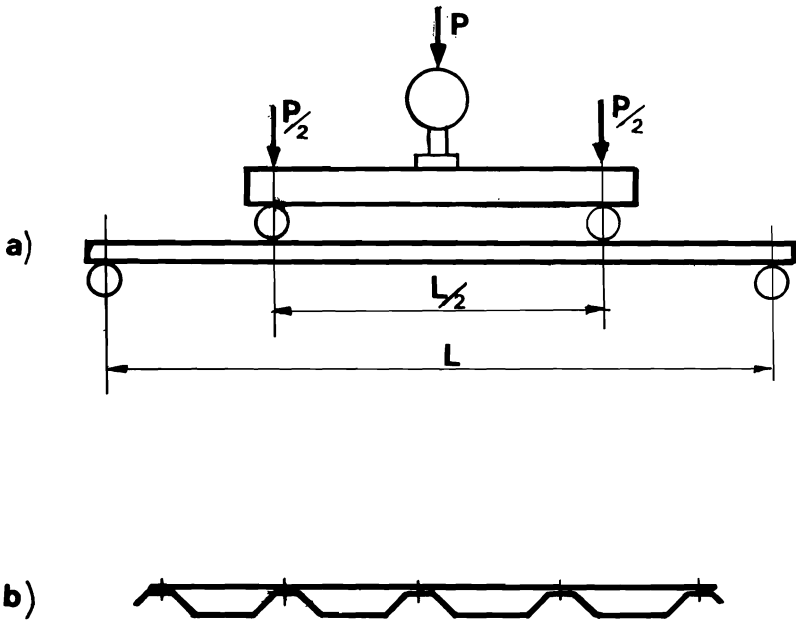


Fig 1 Test Set-up

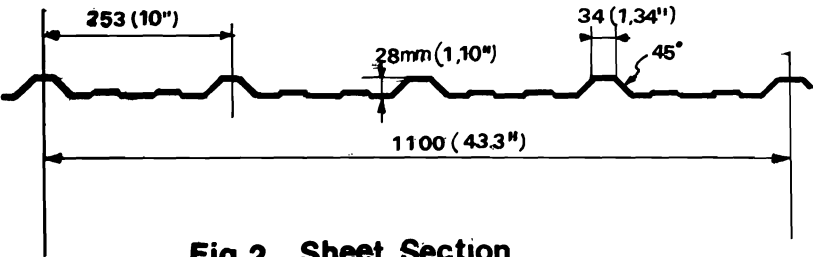


Fig 2 Sheet Section



Fig 3 Flange buckling

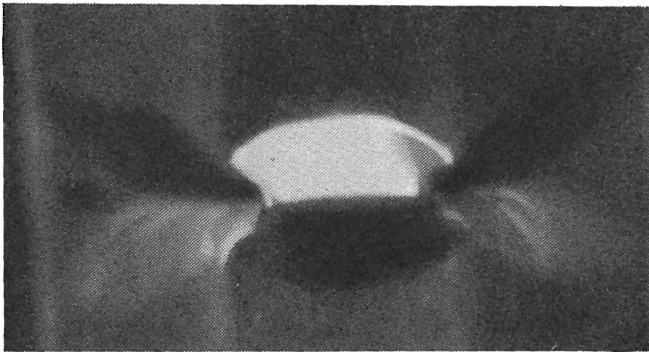


Fig 4 Flange failure

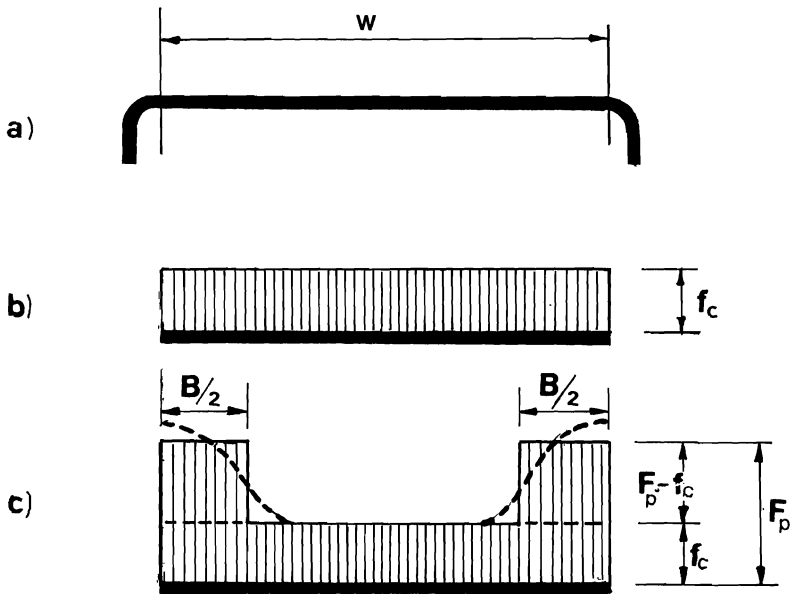


Fig 5 Stresses in flanges

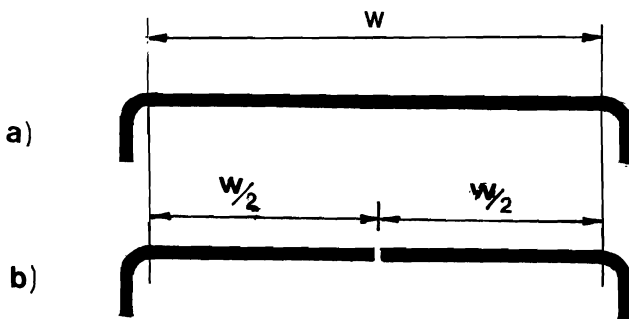
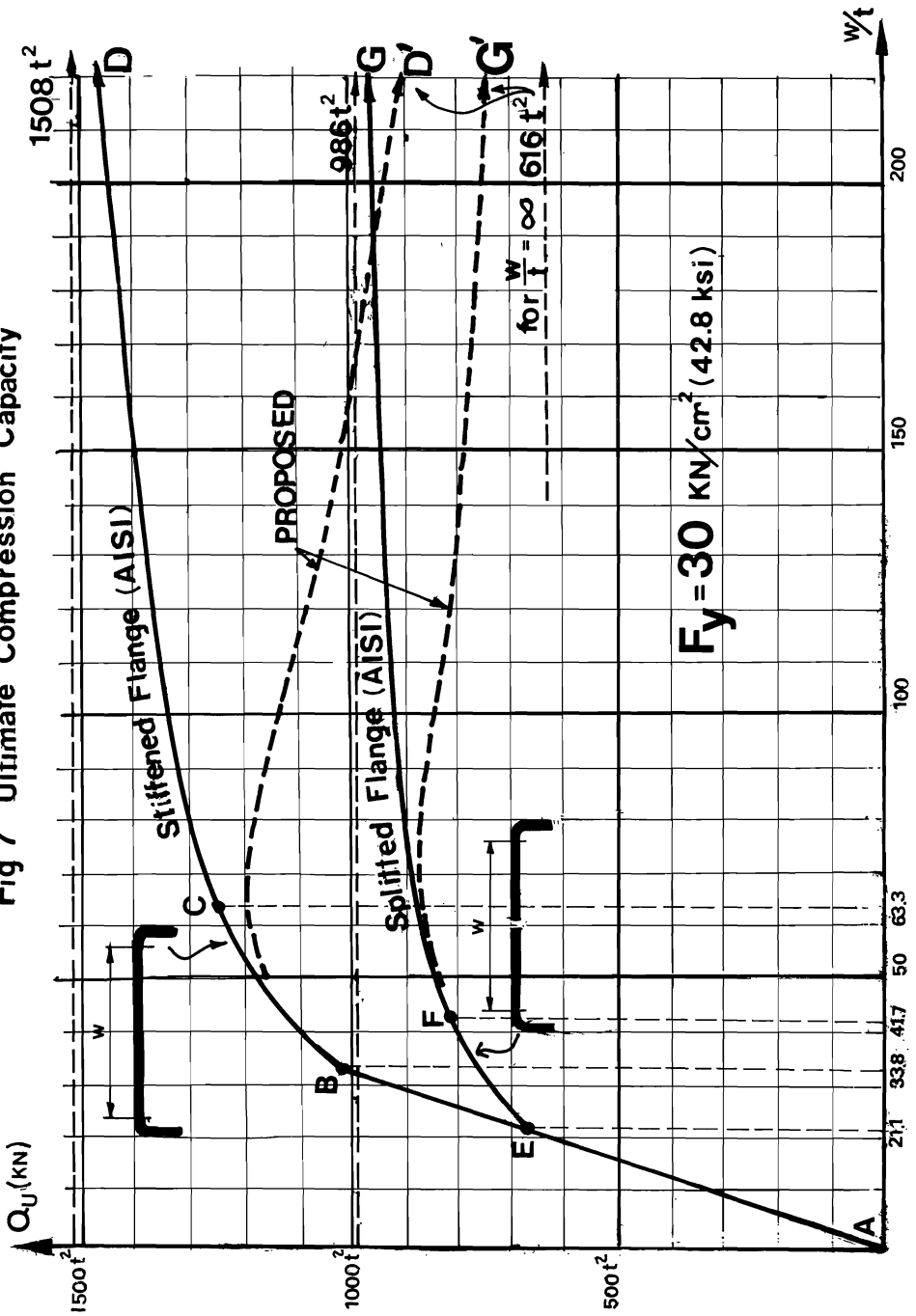


Fig 6 Stiffened and splitted flanges

Fig 7 Ultimate Compression Capacity



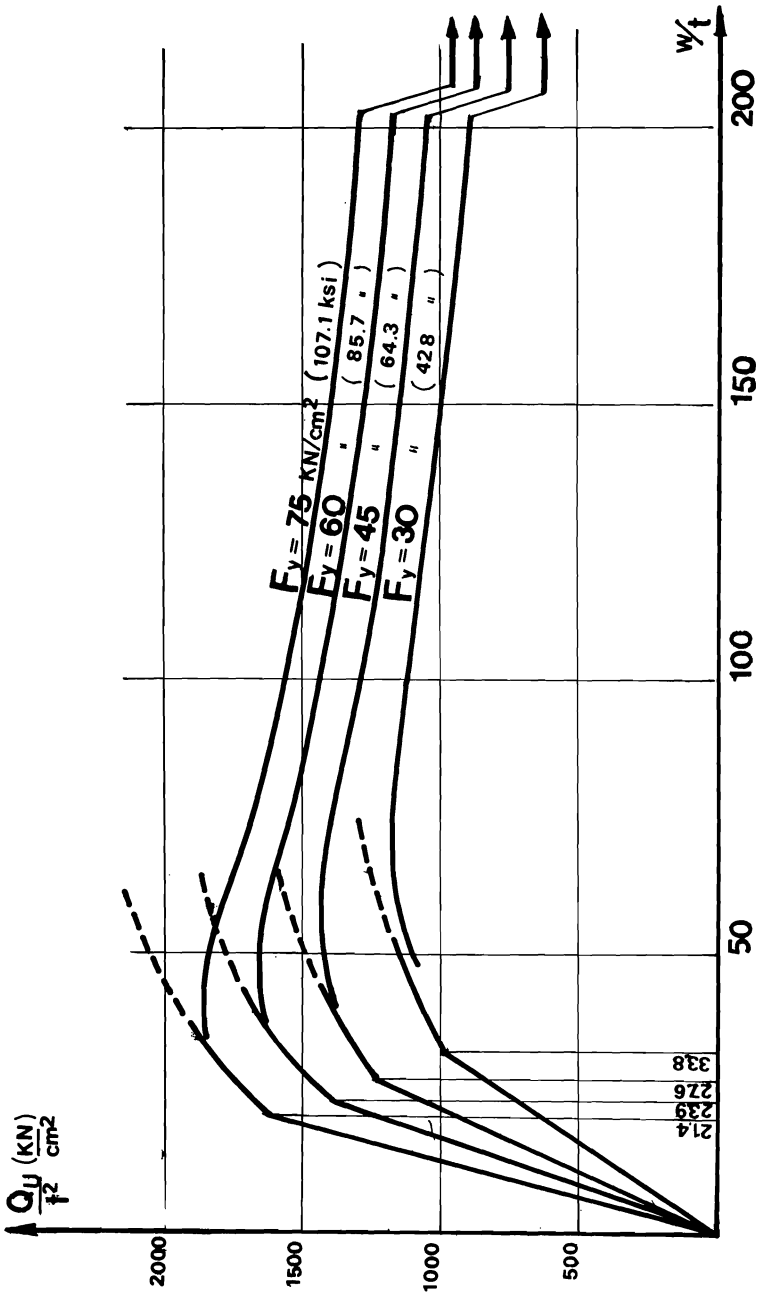


Fig 8 Compression for different Steels

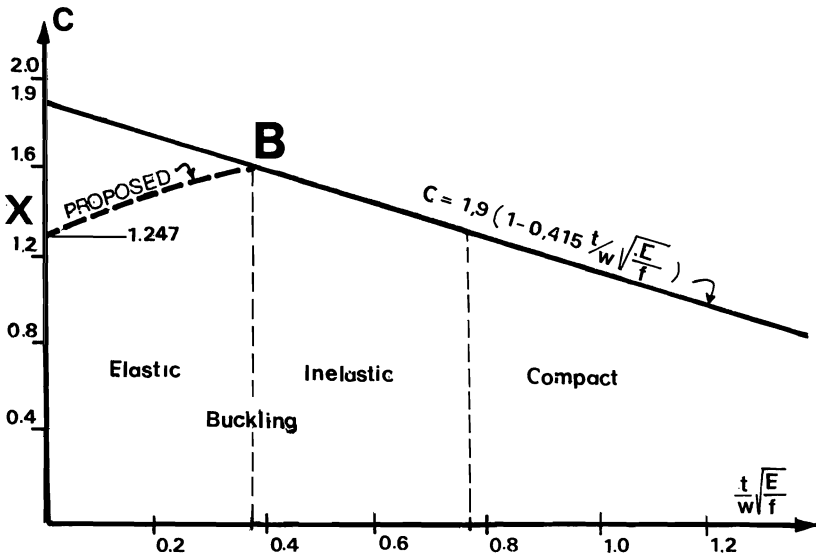


Fig 9 EW as function of the inverse of w/t

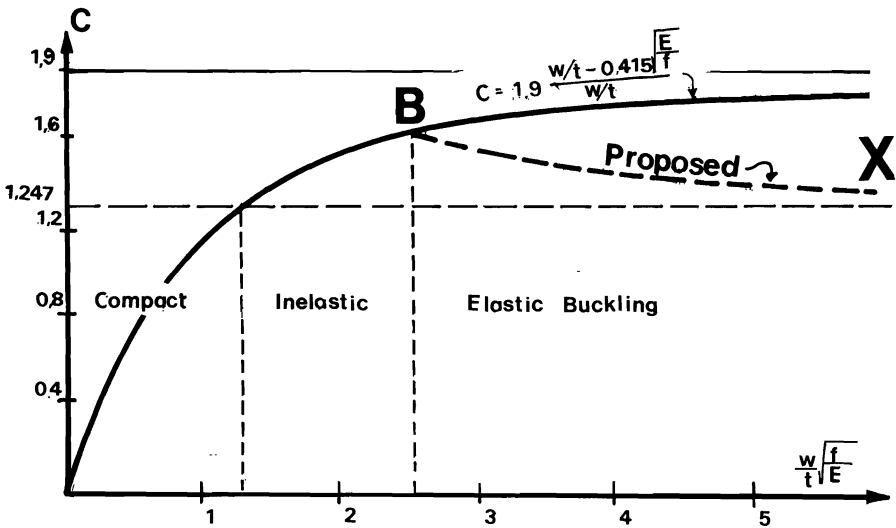


Fig 10 EW as function of w/t

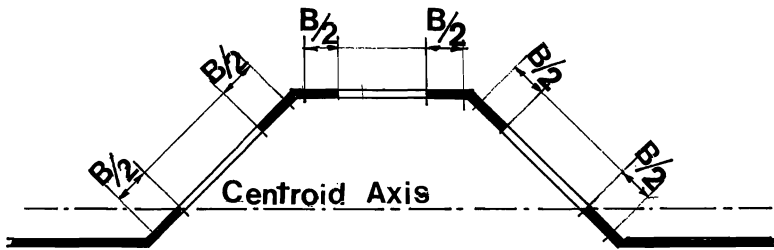


Fig 11 "Real" Effective Section

TABLE 1

t mm	F _y KN/cm	L m	S _e cm/m	P _{ua} KN	N ^o	Put KN	Put Average	$\frac{P_{ua}}{P_{ut}}$
0.40	34.89	4.00	1.75	122.0	B7	88.0	84.0	1.452
					B8	79.0		
					C1	85.0		
0.55	45.97	2.30	2.70	431.7	A15	345.0	342.0	1.262
					A16	339.0		
0.55	36.02	2.30	2.85	357.0	A19	269.0	279.5	1.277
					A20	290.0		

TABLE 2

t mm	F _y KN/cm	L m	S cm/m	S _e ' cm/m	P _{up} KN	N ^o	Put KN	Put Average	$\frac{P_{up}}{P_{ut}}$
0.40	34.89	4.00	2.732	1.307	87.0	B7	88.0	84.0	1.036
						B8	79.0		
						C1	85.0		
0.55	45.97	2.30	3.672	2.072	314.0	A15	345.0	342.0	0.918
						A16	339.0		
0.55	36.02	2.30	3.672	2.274	272.0	A19	269.0	279.5	0.973
						A20	290.0		

